Astron. J. **94**, 1330 (1987)], because there is currently no observational evidence for the existence of such a population.
7. A. L. Cochran *et al.*, *Astrophys. J.* **455**, 342 (1996).
8. M. J. Holman and J. Wisdom, *Astron. J.* **105**, 1987 (1993); M. J. Duncan *et al.*, *ibid.* **110**, 3073 (1995).
9. S. A. Stern, *ibid.* **110**, 856 (1995).
10. P_i is the average collision rate per unit of time and per unit of cross-sectional area of the impacting bodies, multiplied by a factor π [G. W. Wetherill, *J. Geophys. Res.* **72**, 2429 (1967)].
11. P. Farinella and D. R. Davis, *Icarus* **97**, 111 (1992); W. F. Bottke *et al.*, *ibid.* **107**, 255 (1994).
12. D. R. Davis and P. Farinella, *Icarus*, in press. For eccentricities and sines of inclination varying between 0.01 and 0.12, $< P_i >$ and $< V >$ range from 4.21×10^{-21} to 0.62×10^{-21} km^{-2} year^{-1} and from 0.39 to 0.81 km s^{-1}, respectively.
13. D. R. Davis *et al.*, in *Asteroids II*, R. P. Binzel, T. Gehrels, M. S. Matthews, Eds. (Univ. of Arizona Press, Tucson, AZ, 1989), pp. 805–826.
14. E. V. Ryan *et al.*, *Icarus* **94**, 283 (1991).
15. A. Lange and T. J. Ahrens, *Lunar Planet. Sci. Conf.* **XII**, 1667 (1981); S. Kawakami *et al.*, *J. Geophys. Res.* **88**, 5806 (1983); M. J. Cintala *et al.*, *Lunar Planet. Sci. Conf.* **XVI**, 1298 (1985); M. Arakawa *et al.*, *Icarus* **118**, 341 (1996).
16. Initial conditions and model parameters for this case are as follows: The initial population was obtained by joining two power laws for the diameter incremental distribution, with exponents −3.5 for $D < 300$ km and −20 for $D \geq 300$ km, and with 13,000 bodies larger than 300 km. Total initial mass: 3 $M_{\oplus}$. Orbits: $42 < a < 46$ AU; $< e > = 0.05$; and $< \sin i > = 0.05$ (semimajor axis a, eccentricity e, and inclination i). Density: 1.0 g cm^{-3}. Impact strength: 3.0×10^6 erg cm^{-3}. Strength scaling law: energy scaling (size-independent). Fraction f_{KE} of impact energy partitioned into ejecta kinetic energy: 0.1. Exponent of the mass-velocity distribution of fragments: −9/4. Crater mass/projectile energy ratio for cratering impacts: 10^{-8} g erg^{-1}.
17. J. W. Dohnanyi, *J. Geophys. Res.* **74**, 2531 (1969); D. R. Williams and G. W. Wetherill, *Icarus* **107**, 117 (1994).
18. A. L. Cochran *et al.*, *Astrophys. J.* **455**, 342 (1995).
19. P. Farinella *et al.*, *Icarus* **52**, 409 (1982).
20. Several mean motion and secular resonances with Uranus and Neptune are present in the E-K Belt and are associated with chaotic dynamics leading to planet-crossing comet-type orbits [A. Morbidelli *et al.*, *ibid.* **118**, 322 (1996); M. J. Duncan *et al.*, *Astron. J.* **110**, 3073 (1995)].
21. H. F. Levison *et al.*, *Icarus* **108**, 18 (1994).
22. D. Jewitt and K. Meech, *Astrophys. J.* **328**, 974 (1988). For a comparison between shapes of asteroids and fragments from hypervelocity impacts, see V. Catullo *et al.*, *Astron. Astrophys.* **138**, 464 (1984).
23. J. X. Luu and D. C. Jewitt, *Astron. J.* **111**, 499 (1996).

24. P.F. acknowledges financial support from the Italian Space Agency (ASI) and the Italian Ministry for University and Scientific Research (MURST). We are grateful to C. Chapman, H. Levison, F. Marzari, A. Milani, A. Stern, S. J. Weidenschilling, and D. E. Wheeler for useful discussions and comments. This is PSI contribution no. 334.

14 March 1996; accepted 5 July 1996

Penetrative Convection and Zonal Flow on Jupiter

Keke Zhang and Gerald Schubert*

Measurements by the Galileo probe support the possibility that the zonal winds in Jupiter's atmosphere originate from convection that takes place in the deep hydrogen-helium interior. However, according to models based on recent opacity data and the probe's temperature measurements, there may be radiative and nonconvective layers in the outer part of the jovian interior, raising the question of how deep convection could extend to the surface. A theoretical model is presented to demonstrate that, because of predominant rotational effects and spherical geometry, thermal convection in the deep jovian interior can penetrate into any outer nonconvective layer. These penetrative convection rolls interact nonlinearly and efficiently in the model to generate and sustain a mean zonal wind with a larger amplitude than that of the nonaxisymmetric penetrative convective motions, a characteristic of the wind field observed at the cloud level on Jupiter.

During its 57 min of descent into Jupiter's atmosphere, the Galileo probe found that the speed of the zonal flow down to about the 20-bar level was nearly constant with depth (*1*). These results suggest that the zonal jet flows in the atmosphere of Jupiter originate from convection that takes place in the deep H-He interior of the planet (*1*). The alternative view that the zonal winds are driven by the latitudinal gradient of solar heating directly in the atmosphere (thermal winds) and thus do not reflect conditions in the deep interior (*2*) seems less likely because the measured winds do not decay with depth.

One model of the internal structure of Jupiter postulates three major layers: an ice-silicate inner core, a metallic fluid H-He layer, and an outer H_2-He envelope (*3, 4*). In the metallic fluid layer, conduction is considered to be insufficient to carry out all the internal energy because thermal photons are unable to propagate in metallic hydrogen (*5*). Thermal convection probably occurs in this region and generates the magnetic field of Jupiter by dynamo processes (*6*). The H_2-He region is also assumed to be convective (*7*), but the outermost zone, at temperatures around 2000 K or less, may contain radiative and stably stratified layers on the basis of interior models incorporating opacity data on H, He, water, ammonia, and methane (*3, 4*). The temperature lapse rate measured by the Galileo probe suggests that the atmosphere between levels of about 5 and 16 bars may be gravitationally stably stratified (*8*), although this hypothesis cannot exclude the possibility that moist convection may take place in this region (*9*). An essential question relating to the deep origin of Jupiter's zonal flow is then whether the deep thermal convection can penetrate through any outermost nonconvective layer of Jupiter.

Penetrative convection occurs in many situations (*10*) and has been studied in nonrotating plane fluid layers (*10–12*). However, for application to Jupiter, rapid rotation and spherical geometry are necessary, and these have not received much attention in the context of penetrative convection. Nonpenetrative convection with rapid rotation and spherical geometry occurs in columnar structures oriented parallel to the rotation axis (*13, 14*).

Busse (*15, 16*) suggested that a multilayered structure of columnar convection rolls might produce the zonal jets in the jovian atmosphere through nonlinear interactions among the rolls. The viability of this hypothesis has been demonstrated in three-dimensional numerical models (*17, 18*) and laboratory simulations (*19*) of high–Rayleigh number convection in a rapidly rotating Boussinesq fluid shell (*20*). Here we demonstrate that similar processes occur even in the presence of a stably stratified layer, so that Jupiter's zonal jets could have a deep convective origin despite the possible existence of radiative, nonconvective outer layers. We also show how penetrative convection rolls interact nonlinearly and effectively to generate and sustain the zonal flows.

The equation of fluid motion for Jupiter's H-He envelope that rotates with constant angular velocity Ω relative to an inertial frame is

$$\frac{d\mathbf{V}}{dt} + 2\Omega\mathbf{k} \times \mathbf{V} = -\frac{1}{\rho}\nabla p + \mathbf{r}B + \nu\nabla^2\mathbf{V} \tag{1}$$

where $\mathbf{k}$ is a unit vector parallel to Jupiter's rotation axis, $\mathbf{r}$ is the position vector, $\mathbf{r}B$ denotes the small buoyancy force, ν is the kinematic viscosity, ρ is density, $\mathbf{V}$ is the velocity field, and p represents the departure of the pressure from an adiabat. Compressibility and the possible effects of the

K. Zhang, Institute of Geophysics and Planetary Physics, University of California, Los Angeles, CA 90095, USA, and Department of Mathematics, University of Exeter, Exeter, EX4 4QJ, UK.
G. Schubert, Institute of Geophysics and Planetary Physics and Department of Earth and Space Sciences, University of California, Los Angeles, CA 90095, USA.

*To whom correspondence should be addressed.

jovian magnetic field (*21*) are not included.

The velocity field $\mathbf{V}$ can be decomposed into a mean axisymmetric zonal flow $\overline{\mathbf{V}}$ and a nonaxisymmetric (usually with a small scale) convective flow $\tilde{\mathbf{V}}$. The dynamics of the mean flow is mainly characterized by two dimensionless parameters. The Ekman number

$$E = \frac{\nu}{2L^2\Omega} = O\left(\frac{|\nu\nabla^2\overline{\mathbf{V}}|}{|2\Omega\mathbf{k} \times \overline{\mathbf{V}}|}\right) \qquad (2a)$$

measures the ratio of the viscous force $\nu\nabla^2\overline{\mathbf{V}}$ to the Coriolis force $2\Omega\mathbf{k} \times \overline{\mathbf{V}}$. The Rossby number

$$Ro = \frac{V_0}{2\Omega L} = O\left(\frac{|d\overline{\mathbf{V}}/dt|}{|2\Omega\mathbf{k} \times \overline{\mathbf{V}}|}\right) \qquad (2b)$$

measures the relative importance of the Coriolis force and the inertial force $d\overline{\mathbf{V}}/dt$; V_0 is a typical speed of the zonal flow, and L is the corresponding characteristic length scale. Both numbers are small, $E \ll 1$ with any reasonable value of ν and $Ro = O(10^{-2})$ for parameters relevant to Jupiter (*22*), and hence $\overline{\mathbf{V}}$ to a first approximation must be of the form

$$\overline{\mathbf{V}} = F(|\mathbf{k} \times \mathbf{r}|)\frac{\mathbf{k} \times \mathbf{r}}{|\mathbf{k} \times \mathbf{r}|} \qquad (3)$$

which is not affected by the presence of stable layers. Equation 3 implies that the zonal flows must remain largely unchanged in Jupiter's atmosphere and interior along the rotation axis and that $\overline{\mathbf{V}}$ must be nearly symmetric with respect to the equator.

Of course, the Coriolis force cannot sustain $\overline{\mathbf{V}}$. In order to determine the function $F(|\mathbf{k} \times \mathbf{r}|)$, we must go beyond the first approximation by considering the penetrative convection problem. To understand the basic mechanism, we used an idealized rotating spherical shell model (*23*). To show the penetration phenomenon more clearly, we considered a spherical fluid shell thicker (*24*) than that of Jupiter's molecular envelope. In the inner half of the spherical shell, the temperature gradient dT/dr satisfies the condition required for convection

$$\frac{dT}{dr} < 0,\ r_i \leq r < 0.44(r_i + r_o) \qquad (4)$$

while the outer half layer is gravitationally stably stratified

$$\frac{dT}{dr} > 0,\ 0.44(r_i + r_o) \leq r \leq r_o \qquad (5)$$

where r_i and r_0 are, respectively, the inner and outer radii of the shell and T is the departure from the adiabatic temperature (*25*). In our model, the magnitude of the unstable temperature gradient is assumed to be the same order as that of the stable gradient (*25*). In Jupiter, the magnitude of the unstable gradient is likely to be less than that of the stable gradient (*5*). However, a direct comparison of these temperature gradients in the model and in Jupiter is not appropriate because the drive for deep jovian convection is the planet's internal heat loss and not a large superadiabatic temperature.

Because the maintenance of a mean zonal flow can be regarded as a consequence of the nonlinear interaction between nonaxisymmetric convective eddies (*14, 16, 26*), we examined only the relevant penetration phenomenon at the onset of nonaxisymmetric convection (*27*). We first studied a slowly rotating system characterized by $E = 1$ and turbulent Prandtl number $Pr = 1.0$ to illustrate the rotation-related penetration mechanism (Fig. 1A). The convective flow concentrates in the inner convectively unstable region with weak penetration into the outer stable layer, consistent with results in a nonrotating plane fluid layer (*11, 12*). In a slowly rotating or nonrotating system, the amplitude of penetrative convection decreases rapidly in the stably stratified region. Penetrative convection is fundamentally different, however, in a rapidly rotating spherical system like Jupiter. We calculated solutions of rapidly rotating penetrative convection ($E = 10^{-5}$) at two different Pr: a turbulent $Pr = 1$ and a small $Pr = 0.01$. Because radiative diffusion in the outer envelope is much larger than molecular diffusion (*7*), the effective Pr in this region may be quite small if molecular diffusivities apply. In a fast-rotating spherical system, convection rolls penetrate from the inner convective region all the way into the outermost convectively stable layer and, in fact, remain nearly constant in strength along the rotation axis (Fig. 1B). This behavior reflects the most fundamental feature of fluid dynamics in rapidly rotating systems: slow time-dependent motions tend to be two-dimensional.

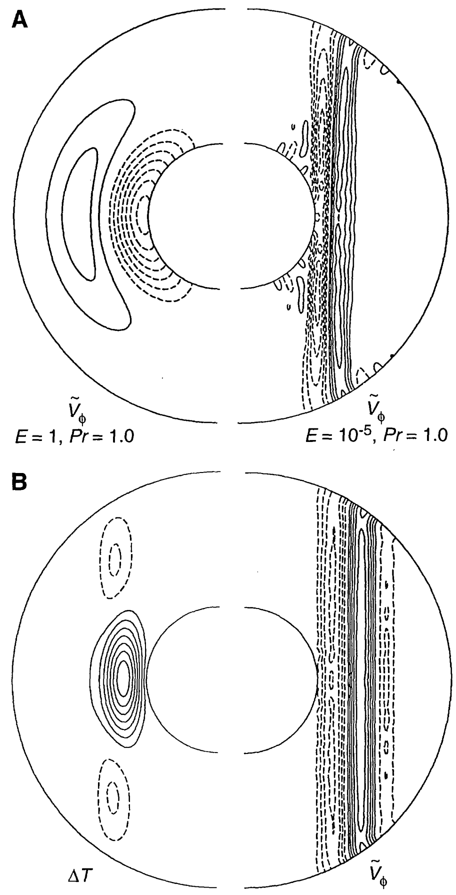

Fig. 1. (**A**) The left side shows contours of $\tilde{V}_\phi$ in a meridian plane in a slowly rotating shell with $E = 1$ and $Pr = 1.0$; the right side is for the case when the system is rotating fast with $E = 10^{-5}$ and $Pr = 1.0$. (**B**) The right side shows contours of the zonal velocity $\tilde{V}_\phi$ in a meridian plane; the left side shows contours of the corresponding temperature perturbation from the basic state for $E = 10^{-5}$ and $Pr = 0.01$. Solid lines denote the eastward flow (positive temperature perturbation) and dashed lines represent the westward flow (negative temperature perturbation). The penetrative feature of rapidly rotating convection is largely unaffected by the size of the Prandtl number. The major portion of the fluid shell is gravitationally stably stratified, which is clearly indicated by the boundary between the positive and negative temperature perturbations.

One can study the maintenance of the mean zonal flow by the penetrative convective motions by taking the average of the azimuthal component of Eq. 1 over a cylindrical surface

$$\frac{dF}{ds} \approx \frac{1}{2\pi\nu}\int_0^{2\pi} \tilde{V}_s\tilde{V}_\phi d\phi \qquad (6)$$

where $\tilde{V}_s$ is the component of penetrative nonaxisymmetric convective flows perpendicular to the direction of rotation and s is the distance from the rotation axis. Equation 6 yields an estimate of the characteristic mean flow speed $|\overline{\mathbf{V}}|_t$ in terms of the amplitude of penetrative convective eddies $|\tilde{\mathbf{V}}|_t$

$$|\overline{\mathbf{V}}|_t \approx \tilde{R}_e\eta_i|\tilde{\mathbf{V}}|_t \qquad (7)$$

where $\tilde{R}_e$ is the local Reynolds number for convective eddies and η_i is the tilt angle of a penetrative convection roll with respect to the radial direction at the equatorial plane, providing a measure of the effectiveness of nonlinear interactions among the rolls (*14*). In the case of perfect rolls in a plane layer, $\eta_i = 0$; however, in a rapidly rotating spherical system with a moderately small Pr, η_i is finite. Hence, the amplitude of $|\overline{\mathbf{V}}|_t$ can be much larger than that of the nonaxisymmetric (eddy) penetrative convection $|\tilde{\mathbf{V}}|_t$ because $(\tilde{R}_e\eta_i) \gg 1$ (*14, 28*).

Penetrative convection rolls can interact strongly in the whole H-He envelope including any outermost stable layer. We achieved an equilibrium state by balancing the Reynolds stress of the penetrative convection rolls against the viscous shear of the mean zonal flow. The alternately directed jets of the mean zonal wind may be a result of additional instabilities when the mean flow $\overline{V}$ is strong, as suggested by three-dimensional numerical simulations (*29*). Because penetrative convection inside the cylinder tangent to the inner sphere's equator requires a much larger temperature gradient to excite, the zonal flow structure in lower latitudes $\phi < 45°$ (determined from the size of the metallic inner core) is fundamentally different from that in higher latitudes. The confinement of the zonal flow jets to the equatorial regions outside the tangent cylinder suggests a rotationally dominated deep convection origin (*15*). Furthermore, the jovian zonal jets are roughly symmetric about the equator and appear to be rather stable, indicating that they are controlled by rotation and deep convection with a long time scale. As a consequence of rapid rotation and spherical geometry, deep convection can readily penetrate through the entire H-He envelope and produce a mean zonal wind with an amplitude that can be much larger than that of the corresponding nonaxisymmetric (eddy) convective flows. Our results on penetrative spherical rotating convection have implications for the dynamics of Earth's fluid core and the sun's convection zone, places where there may be stably stratified layers (*30, 31*).

REFERENCES AND NOTES

1. D. H. Atkinson, J. B. Pollack, A. Seiff, *Science* **272**, 842 (1996).
2. P. J. Gierasch and B. J. Conrath, *J. Geophys. Res.* **98**, 5459 (1993).
3. T. Guillot, D. Gautier, G. Chabrier, B. Mosser, *Icarus* **112**, 337 (1994).
4. T. Guillot, G. Chabrier, P. Morel, D. Gautier, *ibid.*, p. 354.
5. W. B. Hubbard, *Astrophys. J.* **152**, 745 (1968).
6. H. K. Moffatt, *Magnetic Field Generation in Electrically Conducting Fluids* (Cambridge Univ. Press, Cambridge, 1978).
7. D. J. Stevenson and E. E. Salpeter, *Astrophys. J. Suppl. Ser.* **35**, 221 (1977).
8. A. Seiff *et al.*, *Science* **272**, 844 (1996).
9. A. D. DelGenio and K. B. McGrattan, *Icarus* **84**, 29 (1990).
10. B. Straughan, *Mathematical Aspects of Penetrative Convection* (Longman Scientific and Technical, London, 1993).
11. G. Veronis, *Astrophys. J.* **137**, 641 (1963).
12. P. C. Matthews, *J. Fluid Mech.* **188**, 571 (1988).
13. F. H. Busse, *ibid.* **44**, 441 (1970).
14. K. Zhang, *ibid.* **236**, 535 (1992).
15. F. H. Busse, *Icarus* **29**, 255 (1976).
16. ______, *Astrophys. J.* **159**, 620 (1970).
17. Z.-P. Sun, G. Schubert, G. A. Glatzmaier, *Science* **260**, 661 (1993).
18. G. A. Glatzmaier and P. Olson, *Geophys. Astrophys. Fluid Dyn.* **70**, 113 (1993).
19. J. B. Manneville and P. Olson, *Icarus*, in press.
20. F. H. Busse and L. Hood, *Geophys. Astrophys. Fluid Dyn.* **21**, 59 (1981).
21. R. L. Kirk and D. J. Stevenson, *Astrophys. J.* **316**, 836 (1987).
22. Take the typical mean flow speed $V_O = O(100\ \text{m s}^{-1})$, $\nu = 10^{-6}\ \text{m}^2\ \text{s}^{-1}$, $L = O(10^7\ \text{m})$, and $\Omega = 1.76 \times 10^{-4}\ \text{s}^{-1}$ [see, for example, (*7*) and F. M. Flaser, *Icarus* **26**, 280 (1986)].
23. A Boussinesq fluid spherical shell of constant thermal diffusivity κ, constant thermal expansion coefficient α, and constant viscosity ν that is rotating uniformly with a constant angular velocity Ω was assumed. Stress-free and isothermal boundary conditions were also assumed.
24. We have concentrated on the case with the ratio of the inner to outer radius $r_i/r_O = 0.35$. Solutions with other values of r_i/r_O were obtained and show similar features. In our calculation, E is based on the thickness of the shell, $E = \nu/2(r_O - r_i)^2\Omega$.
25. We have used a temperature gradient of the form

$$\frac{dT}{dr} = \frac{3r^*\mathcal{T}}{(n+3)(r_o - r_i)}\left[(r^*)^n - \left(\frac{\beta r_o^*}{r^*}\right)^3\right]$$

where $r^* = r/(r_O - r_i)$ and n, $\mathcal{T}$, and β are parameters. We have focused on the case with $n = 0$ and $\beta = 0.6$. Convection takes place when the Rayleigh number $R = \alpha\mathcal{T}\, g(r_O - r_i)^4/(\kappa\nu)$ is sufficiently large, where g is the acceleration due to gravity; $\mathcal{T}$ measures the magnitude of the driving temperature gradient in the model and determines the vigor of convection through R. The model only qualitatively simulates conditions in the "real" Jupiter.
26. A. P. Ingersoll *et al.*, *J. Geophys. Res.* **86**, 8733 (1981).
27. The linearized Navier-Stokes equation and the heat equation for penetrative convection in a rotating spherical shell are solved. The heat equation is solved analytically in terms of Bessel functions whereas the Navier-Stokes equation is solved numerically by the spectral method.
28. $\tilde{R}_e = (D|\tilde{\mathbf{V}}|_t)/\nu$, where D is the typical length scale of convective eddies. Take $D|\mathbf{V}|_t) = O(10^3\ \text{m}^2\ \text{s}^{-1})$ [B. Fegley and K. Lodders, *Icarus* **110**, 117 (1994)] and $\nu = 10^{-6}\ \text{m}^2\ \text{s}^{-1}$ (*7*), we obtain $\tilde{R}_e\eta_i \gg 1$ for a moderate value of η_i.
29. Z.-P. Sun and G. Schubert, *Phys Fluids* **7**, 2686 (1995).
30. J. A. Jacobs, *The Earth's Core* (Academic Press, New York, 1975).
31. J. P. Zahn, in *Lecture Notes in Physics*, D. Gough and J. Toomre, Eds. (Springer-Verlag, Berlin, 1990), vol. 388, pp. 225–232.

32. The work of K.Z. was supported by the Institute of Geophysics and Planetary Physics, University of California, Los Angeles.

18 April 1996; accepted 3 July 1996

An Archean Geomagnetic Reversal in the Kaap Valley Pluton, South Africa

Paul W. Layer,* Alfred Kröner, Michael McWilliams

The Kaap Valley pluton in South Africa is a tonalite intrusion associated with the Archean Barberton Greenstone Belt. Antipodal paleomagnetic directions determined from the central and marginal parts of the pluton record a geomagnetic reversal that occurred as the pluton cooled. The age of the reversal is constrained by an $^{40}Ar/^{39}Ar$ plateau age from hornblende at 3214 ± 4 million years, making it the oldest known reversal. The data presented here suggest that Earth has had a reversing, perhaps dipolar, magnetic field since at least 3.2 billion years ago.

The behavior of Earth's magnetic field is preserved in the geologic record and can be deciphered with paleomagnetic techniques. With these techniques one can determine the location of the magnetic pole relative to the rock unit at the time the rock cooled through its magnetic blocking temperature. Knowledge of ancient pole positions and magnetic polarities has been used to construct models of plate motion (supercontinent positions and plate velocities) and the geomagnetic dynamo (reversal frequency and intensity). The usefulness of any paleomagnetic pole is determined by the stability of its magnetization (as determined by, for example, stepwise demagnetization, reversal tests, fold tests, or contact tests) and the ability to determine the time when magnetization was acquired. Few records of Earth's geomagnetic field from before 3 billion years ago (Ga) exist. Two early Archean paleopole positions for rocks as old as 3.45 Ga have been reported (*1*), but each study yielded only unipolar directions, with few stability tests. Here, we used paleomagnetic techniques to investigate an Archean tonalite pluton, and our results, when coupled with the results of a detailed geochronologic study (*2*), indicate a 3.2-Ga paleomagnetic pole constrained by reversal and contact tests. Well-documented and dated paleopoles are necessary to construct apparent polar-wander paths, and from these poles minimum average Archean plate velocities can be calculated (*3*).

The Kaap Valley pluton is a circular intrusion 30 km in diameter that forms a valley surrounded by the more mountainous Barberton Greenstone Belt to the north, east, and south (Fig. 1). It is overlain to the west by the early Proterozoic Transvaal Supergroup. The Transvaal Supergroup and related rocks form a thick sequence with an age range from 2552 ± 11 million years ago (Ma) at the base to 2432 ± 31 Ma near the

P. W. Layer, Geophysical Institute, University of Alaska, Fairbanks, AK 99775, USA.
A. Kröner, Institut für Geowissenschaften, Johannes Gutenburg-Universität, 55099 Mainz, Germany.
M. McWilliams, Department of Geophysics, Stanford University, Stanford, CA 94305, USA.

*To whom correspondence should be addressed.